Supplement of Ocean Sci., 15, 615–630, 2019
https://doi.org/10.5194/os-15-615-2019-supplement

Supplement of

Validation metrics for ice edge position forecasts

Arne Melsom et al.

Correspondence to: Arne Melsom (arne.melsom@met.no)

S1 Separation based IIEE displacement metrics

Most definitions were provided in the main text. Here we present some supplementary information which is concerned with metrics $\widehat{D}^{\text{IIEE}}$ that were not included in the recommended set in Sect. 6.3 in the main text.

Provided that the model initialization of the sea ice fraction is close to the observed ice edge fraction at that time, IIEE areas can be expected to emerge as the model ice edge drifts away from the observed edge with an increasing forecast lead time. This evolution is expected to frequently give rise to elongated IIEE areas, and we here adopt the maximum distance inside an IIEE area as the scaling length.

An illustrative example for IIEE and derived metrics is provided in Fig. S1. Here, gray shaded cells represent grid cells in IIEE area ia, while white cells are outside of the IIEE domain. The scaling length l^{ia}_{max} is indicated by the dashed line. Note that when computing the scaling length we have chosen not to include IIEE grid cells with only a single IIEE grid cell neighbour (given by light gray shading in the figure).

Since the definitions of a^{ia} and l^{ia}_{max} take adjacent dry nodes into account, we adopt the hatted notation as introduced in Sect. 2.1 in the main text. The resulting displacement for this area is given as

$$\hat{d}^{ia}_{\text{IIEE}} = a^{ia} / l^{ia}_{\text{max}} \tag{S1}$$

Note that in theory, a node may be adjacent to two IIEE areas. In such cases, we divide the node's area equally between the two relevant IIEE areas.

A solitary IIEE node is formally treated as a separate IIEE area, with scaling length set to the (average) resolution. Furthermore, let A_0 be the total area of the grid cells where the two ice edges overlap. Letting N_A be the number of IIEE areas, we introduce a set of four corresponding displacement metrics here.

1. The root-mean-squared displacement is

$$\widehat{D}^{\text{IIEE}}_{\text{RMS}} = \left[\frac{\sum_{ia=1}^{N_A} a^{ia} \left(\hat{d}^{ia}_{\text{IIEE}} \right)^2}{A_0 + \sum_{ia=1}^{N_A} a^{ia}} \right]^{1/2} \tag{S2}$$

2. The average displacement is

$$\widehat{D}^{\text{IIEE}}_{\text{AVG}} = \frac{\sum_{ia=1}^{N_A} a^{ia} \hat{d}^{ia}_{\text{IIEE}}}{A_0 + \sum_{ia=1}^{N_A} a^{ia}} \tag{S3}$$

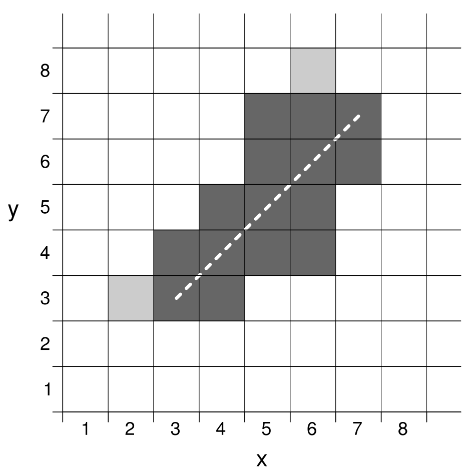

Figure S1. Illustration for scaling length of continuous IIEE areas. Here, the IIEE area is shown as gray shaded grid cells, which in this example is a 17 grid cell area. When determining the scaling length, IIEE area grid cells with only one IIEE area grid cell neighbour are disregarded (light gray shading). The scaling length is then set to the largest distance between the centers of the remaining IIEE area grid cells. This distance is indicated by the white dashed line. The displacement given by Eq. S1 in the metrics defined in Sect. S1 of this continuous IIEE area is then the area (17 grid cells) divided by its scaling length.

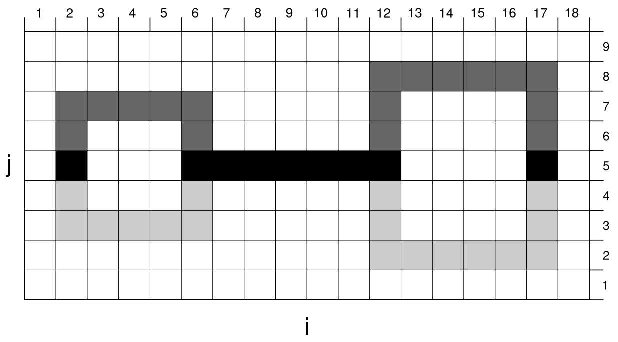

Figure S2. Diagram displaying a sample idealized situation with IIEE areas have taken on the shapes of two rectangles, connected by a straight line where the ice edges in the two products overlap. Here, $w_1 = h_1 = 4$; $w_0 = 6$; $w_2 = 5, h_2 = 6$ where subscripts 1 and 2 correspond to the left and right rectangles, respectively. See the text for details.

3. The displacement bias is

$$\widehat{\Delta^{\text{IIEE}}} = \frac{\sum_{ia^+=1}^{N_A^+} a^{ia^+} \hat{d}_{\text{IIEE}}^{ia^+}}{A_0/2 + \sum_{ia^+=1}^{N_A^+} a^{ia^+}} - \frac{\sum_{ia^-=1}^{N_A^-} a^{ia^-} \hat{d}_{\text{IIEE}}^{ia^-}}{A_0/2 + \sum_{ia^-=1}^{N_A^-} a^{ia^-}} \tag{S4}$$

4. The maximum displacement is

$$\widehat{D_{\text{MAX}}^{\text{IIEE}}} = \max(\hat{d}^{ia}) \tag{S5}$$

In order to shed some light on the relation between the D^{IIEE} metric and $\widehat{D^{\text{IIEE}}}$ we consider an idealized case where two products' ice edges are y symmetric to each other, and form IIEE in the shape of two rectangles, connected by a line where the edges overlap. A sample configuration of such an idealized case is displayed in Fig. S2. Now, take the width (in the x-direction) of the rectangles to be w_1 and w_2 grid cells respectively, while the length of the mutual edge in between is w_0 grid cells. The height of the two rectangles are set to h_1 and h_2 grid cells, respectively.

Then, for $D_{\text{AVG}}^{\text{IIEE}}$ we have

$$\begin{aligned} A^{\text{IIEE}} &= w_1 \cdot h_1 + w_2 \cdot h_2, \\ L &= h_1 + w_1 + w_o + h_2 + w_2 \end{aligned} \tag{S6}$$

where L is the ice edge length for both products. Consequently,

$$D_{\text{AVG}}^{\text{IIEE}} = \frac{w_1 \cdot h_1 + w_2 \cdot h_2}{h_1 + w_1 + w_0 + h_2 + w_2} \tag{S7}$$

To determine $\widehat{D^{\text{IIEE}}}$ we first find that

$$\begin{aligned} \hat{d}_{\text{IIEE}}^{(1,2)} &= w_{(1,2)} \cdot h_{(1,2)} / l_{\text{max}}^{(1,2)}, \\ l_{\text{max}}^{(1,2)} &= (w_{(1,2)}^2 + h_{(1,2)}^2)^{0.5} \end{aligned} \tag{S8}$$

Furthermore, $A_0 = w_0 \cdot 1$, and introducing these quantities into Eq. S3 we find

$$\widehat{D_{\text{AVG}}^{\text{IIEE}}} = \frac{w_1^2 \cdot h_1^2/(w_1^2 + h_1^2)^{0.5} + w_2^2 \cdot h_2^2/(w_2^2 + h_2^2)^{0.5}}{w_0 \cdot 1 + w_1 \cdot h_1 + w_2 \cdot h_2} \tag{S9}$$

Now consider some selected cases:

Case 1 Identical squares, *i.e.*, $w_1 = w_2 = h_1 = h_2 = w;\ \ w_0 = \nu w$. Then,

$$\frac{\widehat{D^{\mathrm{IIEE}}_{\mathrm{AVG}}}}{D^{\mathrm{IIEE}}_{\mathrm{AVG}}} = \frac{1+\nu/4}{1+\nu/(2w)}\sqrt{2} \geq \sqrt{2} \tag{S10}$$

The latter inequality follows since $w \geq 2$. To take an example, assume that the squares have sides with 20 grid cells. Then, if $\nu = 1/4$ (the squares are 5 grid cells apart) the fraction in Eq. S10 is approximately 1.5. If $\nu = 4$ (a separation of 80 grid cells) the fraction has a value of about 3.

Case 2 Different sized squares, *i.e.*, $w_1 = h_1 = w;\ \ w_2 = h_2 = \alpha w;\ \ w_0 = \nu w$. Then,

$$\frac{\widehat{D^{\mathrm{IIEE}}_{\mathrm{AVG}}}}{D^{\mathrm{IIEE}}_{\mathrm{AVG}}} = \frac{1+\alpha^3}{1+\alpha^2}\ \frac{1+\alpha+\nu/2}{1+\alpha^2+\nu/w}\sqrt{2} \tag{S11}$$

Consider the case $\alpha = 1/4$, and set $w = 20$ grid cells. Then, the fraction in Eq. S11 becomes about 1.7 and 2.5 when we set $\nu = 1/4$ and $\nu = 4$, respectively.

Case 3 Identical rectangles, *i.e.*, $w_1 = w_2 = w;\ \ h_1 = h_2 = \delta w;\ \ w_0 = \nu w$. Then,

$$\frac{\widehat{D^{\mathrm{IIEE}}_{\mathrm{AVG}}}}{D^{\mathrm{IIEE}}_{\mathrm{AVG}}} = \frac{1}{\sqrt{1+\delta^{-2}}}\ \frac{1+\delta^{-1}(1+\nu/2)}{1+\delta^{-1}\nu/(2w)} \tag{S12}$$

In the model results, the IIEE areas are usually elongated in the direction parallel to the main direction of the ice edge, *i.e.*, $\delta < 1$. When we investigate the case $\delta = 1/4$ and again set $w = 20$ grid cells, the fraction in Eq. S12 becomes approximately 1.35 and 2.3 for $\nu = 1/4$ and $\nu = 4$, respectively.

Based on these idealized examples, we will expect that the definition of $\widehat{D^{\mathrm{IIEE}}_{\mathrm{AVG}}}$ leads to values that are larger than the corresponding values for $D^{\mathrm{IIEE}}_{\mathrm{AVG}}$. If the results from the idealized examples are representative in operational applications, the ratio of these quantities will be in the approximate range of 1.5-3.

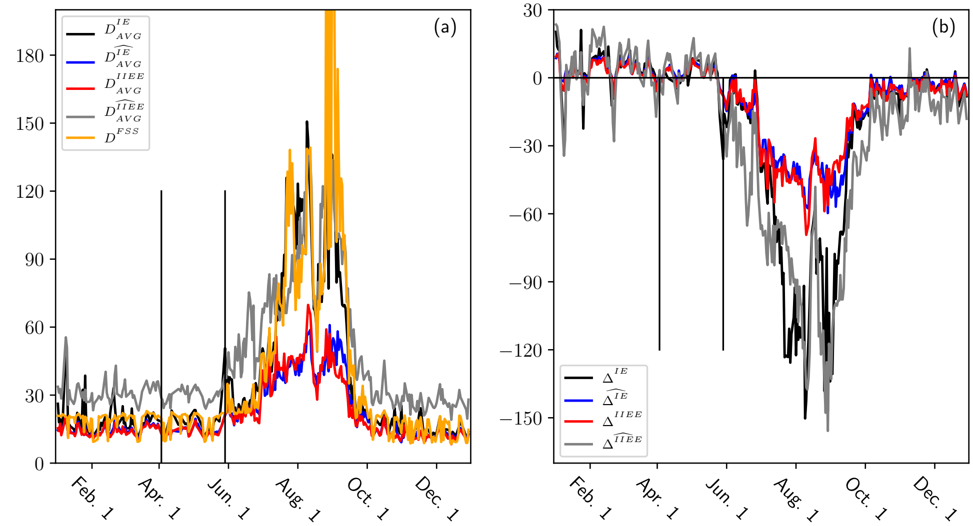

Figure S3. Time series for (a) mean displacement and (b) bias metrics as defined in Sect. 2, for the microwave product *vs.* ice chart data. Vertical lines correspond to the valid time of the two forecasts that were analyzed in Sect. 4. Values along the vertical axes are in units of km.

S2 Comparison of results from ice charts and microwave data

Here we present results from a comparison of the microwave data for sea ice concentration and corresponding results from ice charts, *i.e.*, a comparison of two observational products. The microwave data have been assimilated by the Arctic Ocean Physics Analysis And Forecast product. Differences between assimilated data and the product used for subsequent validation of model results can potentially significantly affect the validation results. Thus, the purpose of this supplementary analysis is to provide information that shed light on the effect of using an independent data set (the ice charts) has on the validation results.

We repeat the analysis in Sect. 5 after having replaced model results with microwave data. The tabulated metric values are provided in Tables S1, S2, and the temporal evolution of average displacement metrics and the displacement biases are

	Ice edge displacement metrics							
	D^{IE}_{AVG}	D^{IE}_{RMS}	D^{IE}_{H}	$\widehat{D^{IE}_{AVG}}$	$\widehat{D^{IE}_{RMS}}$	$\widehat{D^{IE}_{H}}$	Δ^{IE}	$\widehat{\Delta^{IE}}$
Microwave 4-3	14	19	170	13	16	87	1	1
Microwave 5-29	32	68	490	16	20	66	21	4
All microwave data	38	59	350	23	30	110	-26	-13

	FSS		IIEE displacement metrics				
	D^{FSS}	D^{IIEE}_{AVG}	$\widehat{D^{IIEE}_{AVG}}$	$\widehat{D^{IIEE}_{RMS}}$	$\widehat{D^{IIEE}_{MAX}}$	Δ^{IIEE}	$\widehat{\Delta^{IIEE}}$
Microwave 4-3	18	12	28	34	65	0	1
Microwave 5-29	21	15	31	36	74	4	11
All microwave data	40	23	50	56	82	-13	-32

Table S1. Results for the various sea ice edge displacement metrics, when microwave data are compared to ice chart data. Microwave 4-3 and Microwave 5-29 results are metrics valid for 3 April 2017 and 29 May 2017, respectively. All microwave data are averages for all weekly 2017 data, on dates for which results are examined Sect. 5.

	IIEE area metrics		Fractions skill score		
	A^{IIEE}	α^{IIEE}	$n=3$	$n=7$	$n=11$
Microwave 3-4	81	-48	0.68	0.85	0.90
Microwave 5-29	96	1	0.64	0.80	0.86
All microwave data	92	26	0.51	0.68	0.74

Table S2. Supplementary metric scores for microwave data *vs.* ice charts. IIEE area scores are given in units of $1000\,\text{km}^2$.

displayed in Fig. S3. The corresponding results for the model product are given by Tables 3, 4 and Fig. 6. We note the the metrics for average displacements for the microwave product (Fig. S3a) are generally about half of the values when compared to the metrics computed by the model product (Fig. 6a). The exception is the period leading up to the sea ice minimum, when the discrepancy between the two observational products is about the same as revealed by Fig. 6a, and even higher episodically.

Regarding the results for the bias, we note that the ice edge position in the model product is biased negative throughout the year (corresponding to a larger sea ice extent in the ice chart data). When we compare the microwave data with the ice chart, the bias is generally approximately 0, but again large discrepancies between the two operational products are seen in the bias metrics values during the period that leads up to the sea ice minimum.

S3 Map of GODAE regions

The map of GODAE regions in the Arctic Ocean and adjacent seas, which was referred to near the end of the main text, is available as Fig. S4.

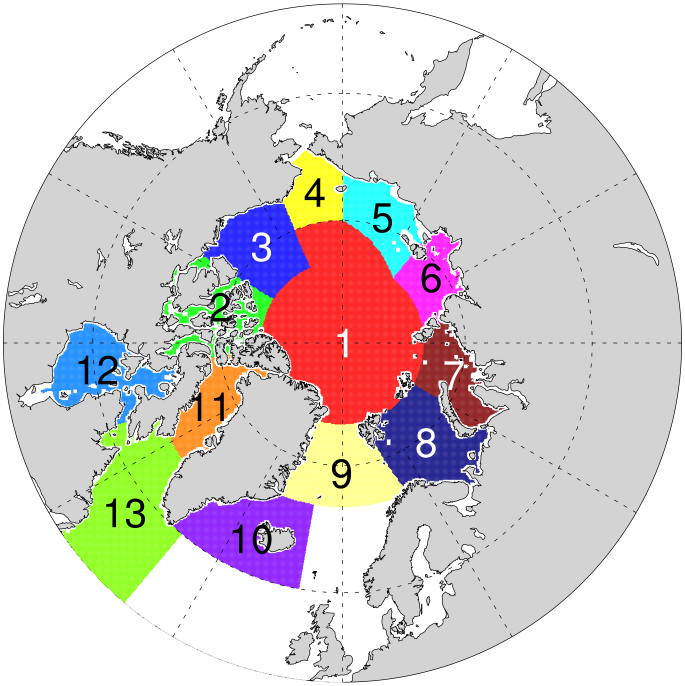

Figure S4. Arctic sub-regions as defined in GODAE OceanView. The numbered regions are (1) Arctic Deep Basin, (2) Queen Elisabeth Islands, (3) Beaufort Sea, (4) Chuckchi Sea, (5) Siberian Sea, (6) Laptev Sea, (7) Kara Sea, (8) Barents Sea, (9) Greenland Basin, (10) Southeast Greenland, (11) Baffin Bay, (12) Hudson Bay, and (13) Labrador Sea.